Gels as emerging anti-icing materials: a mini review

Yizhi Zhuo,[a] *Jianhua Chen,*[b] *Senbo Xiao,*[a] *Tong Li,*[a] *Feng Wang,*[a] *Jianying He*[a] and Zhiliang Zhang*[a]*

[a] NTNU Nanomechanical Lab, Department of Structural Engineering, Norwegian University of Science and Technology (NTNU), Trondheim 7491, Norway.

[b] College of Chemistry, Chemical Engineering and Environment, Minnan Normal University, Zhangzhou 363000, China.

Corresponding Author

*E-mail: jianying.he@ntnu.no; zhiliang.zhang@ntnu.no

This manuscript was accepted by *Materials Horizons*.

https://doi.org/10.1039/D1MH00910A

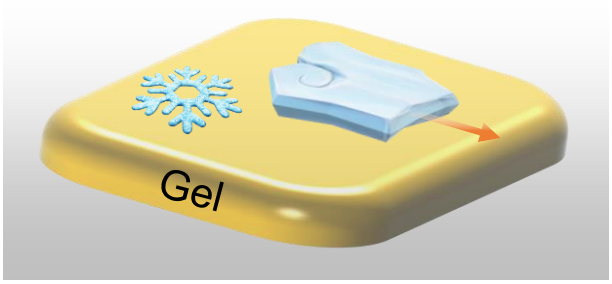

This review summarizes the emerging anti-icing gels and corresponding anti-icing mechanisms, and provides the future perspective.

Abstract: Gel materials have drawn great attention recently in the anti-icing research community due to their remarkable potentials for reducing ice adhesion, inhibiting ice nucleation, and restricting ice propagation. Although the current anti-icing gels are in its infancy and far from practical application due to the poor durability, their outstanding prospect of icephobicity has already shed light on a new group of emerging anti-icing materials. There is a need for a timely review to consolidate the new trends and foster the development towards dedicated applications. Starting from the stages of icing, we first survey the relevant anti-icing strategies. The latest anti-icing gels are then categorized by their liquid phases into organogels, hydrogels, and ionogels. At the same time, the current research focuses, anti-icing mechanisms as well as shortcomings affiliated with each category are carefully analysed. Based upon the reported state-of-the-art anti-icing research and our own experience in polymer-based anti-icing materials, suggestions for future development of the anti-icing gels are presented, including pathways to enhance durability, needs to build up the missing fundamentals, and possibility to enable stimuli responsive properties. The primary aim of this review is to motivate the researchers in both the anti-icing and gel research communities for a synchronized effort to rapidly advance the understanding and making of gels-based next generation anti-icing materials.

Keywords: anti-icing, gels, icephobicity, ice nucleation, ice adhesion

1. Introduction

activities. Frozen water on exposed surfaces of aircrafts, ships, windmills, and powerlines can cause high energy consumption and even catastrophic accidents.[1-3] To ameliorate the detrimental effects of icing, traditional active de-icing methods by using chemicals, heat, mechanical force have been adopted.[4, 5] For examples, anti-freezing liquids are sprayed on fuselage to avoid the freezing of water. Salts are spilled on roads to reduce traffic accidents. Mechanical de-icing of transmission lines is usually applied to prevent collapse and safety problems. However, these traditional methods to remove the accreted ice require periodic operations, high energy input, and/or has negative impacts on both the environment and surfaces.[4, 6] In the last two decades, great efforts have been made to develop passive anti-icing surfaces that can repel water droplets, inhibit ice formation, and reduce ice adhesion strength without external energy inputs.[7-13]

By adopting different strategies, many types of passive anti-icing surfaces have been designed and fabricated.[4] Inspired by the lotus leaf, numerous superhydrophobic surfaces (SHS) have been developed to achieve self-cleaning purpose and liquid repellency.[14, 15] By engineering the hierarchical micro/nano structures, SHS can repel incoming water droplets before freezing at a very low temperature.[16-18] The hierarchical structure can trap air between water droplets and surface to form air pockets, which reduce the heat transfer and therefore retard ice nucleation and growth.[19] Moreover, the trapped air pockets diminish the real contact area between a surface and the eventually formed ice, and serve as crack initiators to promote detachment of ice.[20, 21] As a result, the SHS with trapped air pockets exhibit low ice adhesion strength.[22-26] Nevertheless, air pockets are not always formed on SHS, especially in high humid environment where vapour can condense and freeze inside the surface textures thus leading to mechanical

interlocking and increasing real contact area.[22, 27-29] Even worse, the surface structure can be destroyed during removal of ice or abrasion, thereby rendering loss of icephobicity.[29] To address these challenges, *Nepenthes* pitcher plants inspired liquid infused surfaces (LIS) have been designed and fabricated.[30] The presence of defect-free, slippery liquids at the interface endows the LIS with capability to repel various liquids, maintain low contact angle hysteresis even at high pressure, and lower ice adhesion strength.[30] Unfortunately, due to the high fluidity, the lubricant at the interface can be easily removed by ice and water, resulting in dysfunction of the surface. Although many recent efforts have been made to improve the durability of LIS, they still cannot meet the requirement for practical applications.[31-33] Alternatively, soft coatings have raised interests because of their potential to reach extremely low ice adhesion strength.[34-41] Their softness induces deformation mismatch with ice, which favours the formation of cracks at the interface and thus facilitates the separation of ice from the coating.[36, 40] Although the low modulus of these coatings can enable extremely low ice adhesion, it may lead to weak mechanical durability and unwanted large deformation that can result in dramatic increase of drag force in specific applications, e.g., for wind turbine, aircraft, and ship hull.[4] The drawbacks of these reported anti-icing surfaces call for new and better icephobic materials.

Gels are solid materials consisting of at least one substantially cross-linked network and one liquid. Depending on different liquid parts, the gels can be classified into hydrogels, organogels, ionogels, and hybrid gels, in which water, organic solvent, ionic liquid, and hybrid solvent are the dispersion mediums, respectively. The versatility of gels allows them applicable in many emerging and diverse application fields. For example, hydrogels, which contains large amount of water and tunable networks, have been utilized in contact lenses, tissue engineering, sensors, electrolytes, bio-adhesives,

coatings for medical devices, etc.[42, 43] On the other hand, ionogels possess high electrical conductivity, which enables the utilization as electronic skins,[44] electrolytes,[45] supercapacitors[46] and strain sensors.[47] Thanks to their unique properties in lowering ice adhesion, suppressing ice nucleation, tuning ice growth and restricting ice propagation , gels also emerge as one of the most promising materials for anti-icing purposes very recently.[2, 48-54] Given the extraordinary anti-icing potential, gels deserve dedicated efforts in further research and optimization for their wide acceptance in the anti-icing field. A review is thus in urgent need in order to consolidate the new trends and foster the development towards targeted applications.

Herein, we first present an overview of the icing process, and briefly introduce the state-of-the-art anti-icing strategies. We then outline the latest results of anti-icing gels by categorizing them into organogels, hydrogels and ionogels, with their corresponding icephobic mechanisms, and advantages. Finally, we analyse the shortcomings of current anti-icing gels and propose suggestions for future development. We anticipate that this review can acquaint and motivate the researchers in both anti-icing and gel research communities for rapidly advancing the understanding and fabricating of anti-icing gels.

2. From icing process to anti-icing strategies

In nature, frozen water presents in various forms, including ice, snow, frost, rime, glaze, etc. Ice can be highly threatening to many aspects of human activities. The formation, adhesion, and accumulation of ice on exposed surfaces usually go through nucleation, growth, and then propagation stage. To avoid or ameliorate the hazard from ice accretion, different classes of passive anti-icing surfaces have been developed. Anti-icing strategy is combating icing process by breaking the sequential chain events of ice accumulation.[55] In order to provide an overview of the current design principles of gels

for anti-icing purpose, the state-of-the-art anti-icing strategies are summarized based on the stages of icing in this section, as shown in Fig. 1 & 2. Specifically, collection of water, ice nucleation, ice growth and recrystallization, and ice propagation via frost halos and inter-droplet ice bridging, are highlighted on the left panel of Fig. 1 (light green background), while the corresponding anti-icing strategies are shown on the right panel (light orange background).

2.1. Avoiding adhering of liquid water

The most commonly observed unwanted icing on exposed surfaces starts from pre-existing water that is collected via condensation[56] (Fig. 1a, left) or adhesion of impacting water droplets (Fig. 1a, right).[16]

Removing the water before ice nucleation is a direct way to avoid unwanted ice accumulation. To repel liquid water, various types of surfaces have been developed. SHS comprise hierarchical micro/nano structure and a low surface energy layer, showing ultra-high water contact angle (WCA $\geq$ 150 °C) and low contact angle hysteresis (CAH $\leq$ 5 °C). Therefore, they can repel incoming water droplets, thus preventing icing on their exposing face (Fig. 1b, left).[6] Since dynamic wetting behavior of water droplets on SHS directly relates to anti-icing performance, Mishechenko et al. investigated the behavior of dynamic droplets impacting SHS, and revealed that hydrophobic polymeric coatings with closed-cell surface microstructure exhibit enhanced mechanical and pressure stability.[6] Wang et al. showed that the stability and water/ice repellency of SHS can also be improved by integrating zinc oxide nanohairs onto flexible poly(dimethylsiloxane) (PDMS) micropapillae.[13] The nanohairs improve the water repellency, while the flexible PDMS cushions the droplets impacting.

Another example is LIS, which shows low CAH due to the high fluidity of the water-immiscible slippery liquid (Fig. 1b, right).[30] By proper design, even lower water sliding angles than those observed on SHS were reported.[57] The slippery liquid at the interface can not only avoid the adhering of liquid water but also lower the ice adhesion strength when ice forms on the surface.

2.2. Inhibiting ice nucleation

Nucleation is a probabilistic event and the first step of icing, which is also the rate-limiting step for ice formation.[55] Ice nucleation generates new liquid-solid interfaces, which requires a certain degree of subcooling to overcome the free energy barrier.[58, 59] As shown in Fig. 1c, the formation of ice nucleus can be either through homogeneous nucleation or by heterogeneous nucleation, where homogeneous nucleation takes place within the liquid phase away from foreign surfaces, while heterogeneous nucleation initiates at the liquid-solid interface.[59] The relationship between heterogeneous and homogeneous nucleation can be expressed as,[58]

$$\Delta G_{\text{het}} = f(\theta_{\text{iw}}, R)\Delta G_{\text{hom}} \quad (1)$$

where ΔG_{het} and ΔG_{hom} are the Gibbs free energy barrier for heterogeneous nucleation and homogeneous nucleation, respectively. Specifically. $f(\theta_{\text{iw}}, R)$ is a geometric factor and ranging from 0 to 1, meaning that the free energy barrier for heterogeneous nucleation is usually lower than that for homogeneous nucleation in the same system. θ_{iw} and R are the contact angle of ice-water and the roughness curvature radius, respectively. In addition, the ΔG_{hom} can be described by,[55, 60]

$$\Delta G_{\text{hom}} = \frac{16\pi\gamma_{\text{iw}}^3}{3\Delta G_{\text{f,v}}^2} \quad (2)$$

where γ_{iw} and $\Delta G_{f,v}$ is the ice-water interfacial tension and the volumetric Gibbs free energy difference between the bulk ice and bulk water, respectively.

The physics of heterogeneous nucleation can be described by classical nucleation theory, which expresses the rate of nucleation as:[60]

$$J(\mathrm{T}) = K(T)\mathrm{A}\exp\left(\frac{-\Delta G(T)}{\mathrm{k_B}T}\right) \quad (3)$$

where $K(T)$ is a kinetic prefactor representing the diffusive flux from free water molecules across the icing front interface; A, $\Delta G(T)$, $\mathrm{k_B}$, and T denote the droplet-substrate contact area, the Gibbs free energy barrier, Boltzmann constant, and substrate temperature, respectively.

Since the free energy barrier for heterogeneous nucleation is usually lower than that for homogeneous nucleation in a given system, ice nucleation usually starts from foreign surfaces (heterogeneous). The ability to inhibit ice nucleation is usually evaluated by the nucleation delay time, which is inversely proportional to the nucleation rate, $\tau = J(T)^{-1}$. Equations (1-3) show that there are several ways to inhibit heterogeneous ice nucleation: 1) decreasing the droplet-substrate contact area; 2) increasing the energy barrier by tunning the roughness curvature radius, the ice-water interfacial tension, and the volumetric Gibbs free energy difference between the bulk ice and bulk water. For example, Bai et al. used graphene oxide nanosheets with controlled sizes in water droplets to probe the critical ice nucleus size and demonstrated that the graphene oxide with size smaller than the critical ice nucleus can lead to a much higher free-energy barrier for nucleation, namely inhibiting the nucleation promoting effect of the graphene oxide.[61] Eberle et al. also showed that ice nucleation can be inhibited by tuning surface roughness and minimizing the droplet-substrate contact area (Fig. 1d, left).[60] They fabricated micro-nano hierarchical structure with micro pillars and nanopits, which reduced the droplet-

substrate contact area. In addition, the prepared surfaces showed ultrafine roughness, which promoted the formation of a confined interfacial quasi liquid layer between ice nuclei, leading to a change of θ_{iw}. As a result, the prepared surface exhibited a remarkable delayed ice nucleation time of 25 hours at -21 °C. Yang et al. prepared supercharged polypeptides (SUPs) surfaces to tune ice nucleation (Fig. 1d, right).[9] They found that negatively charged SUPs inhibited ice nucleation, while positively charged SUPs promoted nucleation. It was shown that the local electric field near charged surfaces affected the water-ice nucleus interfacial tension and the volumetric Gibbs free energy difference between the bulk ice and bulk liquid and thus changed the energy barrier.

2.3. Controlling ice growth

Ice nucleation generates ice crystals, which form an opaque slushy mixture with the remaining liquid, followed by ice growth. Taking the freezing process of water droplets on normal surfaces as an example, as the latent heat is released through the highly conductive droplet-substrate interface, ice grows isothermally, initiating from the interface and forming a distinct pointy tip at the end (Fig. 1e).[62] During the ice growth process, the volumetric ice growth rate can be estimated by:[48]

$$\dot{V} \propto \dot{Q} \propto \frac{\Delta T}{R} = \frac{T_m - T_e}{R} \quad (4)$$

where $\dot{Q}$, ΔT, and R are the heat flux, temperature difference between melting temperature (T_m, 0 °C for pure water) and substrate/environment temperature (T_e), and thermal resistance between substrate/environment and the freezing front, respectively. The growth direction is inverse to the major heat release direction.

The time for completing ice growth is usually orders-magnitude shorter than ice nucleation delay time. Thus, there are only few studies reported on prolonging the ice

growth time. According to equation (4), the ice growth rate is related to the environmental temperature and the thermal resistance between environment and freezing front. It means that the ice growth time can be increased by enhancing the thermal resistance of the heat release channel. For example, Shen et al. demonstrated that the micro-nanoscale hierarchically structured superhydrophobic surface not only inhibited ice nucleation due to the decreased actual solid-liquid contact area, but also lowered the ice growth rate owing to the insulating action caused by the trapped air pockets.[19]

Notably, because ice growth direction is opposite to the major heat release direction, the growth direction can also be altered by changing the temperature difference. By controlling substrate temperature and increasing heat convection, ice can grow from the droplet-air interface to droplet-substrate interface, leading to the so-called self-dislodging of formed ice (Fig. 1f).[63] However, such phenomenon requires artificial control of the substrate temperature and environmental condition, which is not appliable in realistic situation.[48]

In addition, the wettability of solid surface also influences the pattern of ice growth in the condensation-frosting process.[64] Liu et al. reported the successful controlling of ice growth by altering the wettability of solid surface.[64] On a hydrophilic surface, ice favoured an along-surface growth mode due to the presence of bilayer hexagonal ice with an optimized matching basal face and thus promoted rapid ice growth rate. Whereas ice on a hydrophobic surface showed an off-surface growth mode, which resulted in weak adhesion between the formed ice crystals and the solid surface.

2.4. Restricting ice propagation

The coverage of ice on a surface is usually realized through the inter-droplet interactions rather than individual freezing of droplets. This process is the so-called ice

propagation. The freezing of a droplet can initiate ice propagation via either frost halos or inter-droplet ice bridging. To avoid ice covering a whole surface when the water droplet freezing is inevitable, ice propagation should be restricted.

Frost halos is a phenomenon that occurs during freezing of a droplet. The latent heat during ice nucleation is released to the remaining liquid, thus induces its evaporation. Due to the lower temperature of the substrate, vapor can subsequently condense or even freeze on the substrate close to the frozen droplet (Fig. 1g).[65] Those frost halos may render the freezing of nearby droplets through a domino effect. Alternatively, the explosive latent heat will also be released through the substrate, which mitigates the evaporation of remaining liquid. As such, increasing the thermal conductivity of the substrate can suppress the frost halos and minimizing the ice propagation.[65, 66] Jung el al. already revealed that higher thermally conductive surfaces can form a smaller frost halo due to the faster removal of latent heat, and thus have lower possibility of freezing of neighbouring droplets (Fig. 1h).[65]

Inter-droplet ice bridging is another phenomenon that could lead to ice propagation.[55] The saturated vapor pressure over frozen droplets is lower than that over liquid droplets at the same subfreezing temperature, resulting in localized vapor pressure gradients in the system where the frozen droplets serve as local humidity sink.[55] In addition, the heat released by freezing will conduct to the neighbouring droplets via substrate, leading to the localized temperature gradients.[67] Both localized vapor pressure gradients and temperature gradients cause the mass transfer from liquid droplets to the frozen one, namely the water molecules evaporate from the liquid droplets and then deposit on the frozen droplets. As shown in Fig. 1i, during this process, the frozen droplet grows towards the adjacent liquid droplets that are being harvested, forming ice crystals.[55, 68] The liquid droplets will start freezing once the formed ice crystals contact to them,

forming ice bridges to connect droplets to form a network. However, the ice bridge will fail when the distance between the edge of the frozen droplet and the centre of the liquid droplet (L_{max}) larger than the original diameter of the liquid droplet (d), leading to a dry zone.[68]

The way to break ice bridging is to control the distance between the frozen and unfrozen droplets. As discussed previously, the ice bridge will fail when the distance between the edge of the frozen droplet and the centre of the liquid droplet (L_{max}) is larger than the original diameter of the liquid droplet (d). The frozen droplets will harvest the neighbouring water droplets and thus create an annular dry zone around the formed ice. Spatially controlling ice formation through surface patterning, wettability tunning, and polymer grafting can fail the inter-droplet bridging and create large ice-free areas (over 90% of the exposed surface).[67, 69-71] For example, Ahmadi et al. have designed aluminium surfaces with microgrooves for reserving water, which can freeze to "ice stripes" in chilled conditions (Fig. 1j, top).[69] The "ice stripes" harvest water vapor in the nearby regions and then leaves the surface with more than 90% of ice-free area. On surfaces with macrotexture[70] and microgroove patterns[71], an increasing gradient of water vapor concentration from the bottom to the top of the surface topography can be formed thanks to the local structural confinement effect. Thus, vapor condensation and frost formation are preferential on the upper tips of the surface structure. The formed frost constantly collects vapor from the condensed droplets in the local valley due to the vapor pressure difference, and consequently breaks the inter-droplet bridging and stop ice propagation. Ice propagation can also be guided by tailored surface local properties. Jin et al. prepared patterned polyelectrolyte coatings to inhibit condensation freezing (Fig. 1j, bottom).[67] The prepared poly[2-(methacryloyloxy)-ethyltrimethylammonium iodine] brushes on the surface promoted ice nucleation, leading to the earlier formation of ice

on the grafted area. Due to the low vapour pressure over ice, water vapour favoured depositing on the formed ice. In addition, during the freezing process, the latent heat was released to the substrate, facilitating the evaporation of neighbouring water droplets. For the best result, an ice-free zone up to 96% of the whole surface area can be achieved.

2.5. Reducing ice adhesion

After formation of ice, the most effective strategy to ameliorate the hazard from ice accretion is to reduce ice adhesion, and in an ideal case letting the formed ice be automatically removed by natural forces, e.g., gravity, wind. From different scales, ice adhesion can be described by intrinsic and macroscopic adhesion, as shown in Fig. 2a.[4] Intrinsic adhesion is a result of the atomistic attraction of water/ice molecules to a surface in the form of coulombic and van der Waals forces.[72-75] The origin of intrinsic adhesion implies that the following methods can be used to reduce ice adhesion: 1) to weaken the atomistic interactions between the surface and water molecules by lowering the surface energy and increasing the hydrophobicity of the surface; 2) to destabilize the contact between surface and water molecules by introducing insulating layer. Meuler et al. have shown that ice adhesion strongly correlates with water wettability ($\tau \propto 1 + \cos\theta_{rec}$, where τ and θ_{rec} are ice adhesion strength and water receding contact angle, respectively).[76] Although the correlation fails for surfaces with ice adhesion strength larger than 60 kPa, it demonstrates the possibility to tuning ice adhesion by the method 1).[77] To lower the surface energy, fluorine-containing polysiloxanes are usually chosen as the coating materials.[4, 78] LIS as an example for method 2), can lower ice adhesion since the slippery liquid layer serves as a barrier to avoid the direct contact of ice and substrate.[30] LIS can be fabricated by infusing different lubricant (silicone oil,[79] perfluoroalkylether,[80] liquid paraffin[31]) into porous structure or polymeric networks. The

abundant lubricant forms a stable, defect-free, and slippery layer, which serves as an insulating layer between ice and the substrate. The slippery nature of infused lubricant grants prepared surface with low adhesion to ice.

Given that real surfaces are usually rough on different length scales, there are always voids at the ice-surface interface. These voids can function as crack initiators, create stress concentration, and thus affect the interface crack propagation. Macroscopic adhesion is thus a function of the intrinsic adhesion and interface cracks. According to fracture mechanics, the critical strength to separate two solid surfaces can be approximated as: $\tau = \sqrt{EG/(\pi a \Lambda)}$, where E, G, a, and Λ are the elastic modulus, surface energy, crack length and a non-dimensional constant related to geometric configuration, respectively.[36, 38, 81] The equation indicates that tuning the features of voids by altering surface roughness and controlling deformation incompatibility (such as modulus mismatch between ice and surface[40] as well as modulus mismatch in different regions of surface[36, 82]) can also reduce the ice adhesion strength. For examples, due to the presence of micro/nano surface structures, some SHS can not only reduce the contact areas/points controlled by intrinsic adhesion but also facilitate the initiation and propagation of interface cracks.[20, 21] The prerequisite for those SHS with reduced ice adhesion is the existence of Cassie wetting state, which is affected by the size and topography of the micro-voids (Fig. 2b). Alternatively, designing and controlling the properties and morphologies of sub-surface structures can promote the formation of interface cracks and significantly lower ice adhesion strength.[34, 36, 37] As shown in Fig. 2c, He et al. prepared soft PDMS coating with macroscale substructures under the surface.[36] The presence of the macroscale substructures facilitated the formation of voids at the interface because of deformation incompatibility, resulting in a super-low ice adhesion strength (5.7 kPa). Coincidentally, Irajizad et al. introduced ultrasoft gel fillers into

PDMS matrix to achieve modulus mismatch in different surface regions, which render stress localization and deformation incompatibility during de-icing.[82]

3. Anti-icing gels

Based on the above analyses of icing processes and anti-icing strategies, it can be easily seen that gels have great potential to be used as anti-icing materials. First, the large amount of liquid existing in the gels offers the possibility to form an interfacial liquid layer which naturally weakens the intrinsic ice adhesion.[83, 84] Second, its low surface elastic modulus can induce a distinct stiffness mismatch between ice and substrate which promotes the initiation of interface cracks and thus drastically lower the ice adhesion strength.[40, 41] Moreover, the versatility of the available liquids and cross-linked networks provide many alternatives for controlling ice nucleation, ice growth and even ice propagation. The physical properties of gels are usually dominated by the species of their liquid part, e.g., hydrogels are often hydrophilic because of the abundant water; ionogels display high electrical conductivity due to the presence of conductive ionic liquid. Therefore, in the following, we summarize the performances and mechanisms of current anti-icing gels by their liquid base, *i.e.*, organogels, hydrogels, ionogels.

3.1. Organogels

The large amount of organic liquids inside organogels leads to extremely low density of elastic strands and elastic modulus values 2-3 orders of magnitude lower than that of ice.[4, 85] The giant modulus mismatch between organogel and ice grants those gels ultralow ice adhesion due to the deformation incompatibility during de-icing(Fig. 3a).[40] As shown in Fig. 3b, Beemer et al. prepared gels consisting of cross-linked PDMS

networks and different amount and molecular weight of non-reactive trimethyl-terminated PDMS (t-PDMS).[40] The results showed that ice adhesion follows $\tau = \sqrt{W_{\mathrm{adh}}\mu/t}$, where W_{adh}, μ, and t are the work of adhesion between ice and coating, shear modulus and thickness of coating, respectively. They also demonstrated the formation and propagation of air cavity at the ice-coating interface. Although the PDMS gels exhibit ultralow ice adhesion strength, the low modulus may lead to weak mechanical durability and the unwanted large deformation during specific applications, e.g., for wind turbine, aircraft, and ship hull.[4]

The other functionality of organogel for anti-icing is their lubricant-secretion ability. The crosslinking reaction of PDMS in the presence of other organic liquids can lead to an increase of the free energy of mixing (ΔG_{mix}), and resulting in demixing of organic liquid and PDMS matrix (if $\Delta G_{\mathrm{mix}} > 0$).[84] As shown in Fig. 3c, the syneresis effect continuously generates a liquid layer on the topmost of the prepared organogel surfaces under certain conditions. The formed liquid layer can serve as an insulating layer to mitigate the intrinsic adhesion, consequently, achieving extremely low ice adhesion (*ca.* 0.4 kPa).[84] Such a low ice adhesion enables the autonomous sliding of ice pillar off a slightly inclined surface. The organogel reported above is prepared by an *in-situ* method, in which cross-linking and infusing occur at the same time. Post-infused method, infusing lubricant after cross-linking, can also be applied to prepared organogel with ultra-low ice adhesion strength. Wang et al. demonstrated that liquid paraffin can be infused into cross-linked PDMS networks at an elevated temperature.[83] After cooled down to room temperature, the surface of prepared organogel was covered by a thin layer of paraffin, which is released from the bulk PDMS networks due to the osmotic pressure driven by the temperature change. The continuous release of paraffin makes the organogel displays ultra-low ice adhesion even after 35 icing/deicing cycles and 100

days environmental exposure. By incorporating such thermoresponsive property into organogel, other surfaces with switchable interfacial properties are designed and fabricated for anti-icing applications.[52, 86] Urate et al. used micro/nanostructured moulds to prepare textured organogel films consisting of cross-linked PDMS as the matrix and polymethylphenylsiloxane (PMPS) as the lubricant.[86] By tuning the ratio of PMPS and PDMS, the critical syneretic temperature (CST) can be varied from -15 to 50 °C. When the temperature is lower than CST, PMPS is spontaneously secreted to the topmost layer of the gel, forming a slippery surface, which contributes to excellent icephobic performance. In the meantime, PMPS on the surface gradually absorbs into the polymer networks when temperature is above CST. The release of oil also induced a change of optical properties since the released oil can bury the surface micro/nanotextures. By infusing a binary liquid mixture with an upper critical solution temperature into a polymer network, Ru et al. fabricated a reversibly thermoresponsive organogel (Fig. 3d).[52] The critical phase separation temperature was tuned by varying the composition. Due to the phase separation ability during temperature change, the organogels can reversibly secrete/absorb liquid, and thus exhibit a switchable lubricating property. The organogel in lubricating state showed extremely low ice adhesion (<1 kPa).

Although the above organogels with lubricant surface present ultralow ice adhesion, the easy depletion of liquid lubricant may pollute the environment and lead to poor durability. To improve the durability of anti-icing organogels, liquid lubricants can be replaced by solid organic ones, which mitigate the loss of sacrificial layer.[87, 88] Following such concept, alkane[88] and perfluoroalkane[87] have been infused into PDMS matrix at temperature higher than their melting points. During the infusing process, sufficient amount of solid lubricant will cause the swelling of the elastomer matrix, and then induce the gradient of both the concentration and the stress after cooling down to room

temperature or even lower temperature. As a result, the solid lubricant inside the elastomer matrix can be squeezed out to the topmost surface layer when the top sacrificial layer is being damaged or removed (Fig. 3e).[88] The solid nature and regenerability synergistically improve the durability of the prepared organogel. Despite the durability of solid organogels have been greatly improved, the consumption of lubricant will eventually render the loss of icephobicity.

By incorporating dynamic bonds into the polymer networks of an organogel, new functionality, *i.e.*, self-healing, can be obtained to further improve the mechanical durability.[89, 90] Due to the reformation ability of the broken dynamic bonds (hydrogen bonds, disulfide bonds, metal-ligand coordination etc.), the prepared organogels can repair mechanical cuts and scratches. It should be noted that the presence of liquid medium in supramolecular networks can accelerate the chain mobility, and thus promote the reconstruction and reversible exchange of dynamic bonds, leading to a high self-healing efficiency.[89]

3.2. Hydrogels

Hydrogels contain large amount of water, which has freezing point around 0 °C (at normal atmosphere). Therefore, common hydrogels usually show poor freezing resistance to low temperature. However, by introducing additives and modifying the polymer networks, hydrogels can maintain their softness and other gel characteristics at sub-zero temperatures.[91] The modified hydrogels are the so called anti-freezing hydrogels. It is envisaged that anti-freezing hydrogels also work for anti-icing purpose since the interfacial non-frozen water can not only serve as lubricant for lowering ice adhesion but also tune ice formation, including ice nucleation and ice propagation.[2, 49-51]

These hydrogels can be categorized by their synthesis strategies, *i.e.*, 1) introduction of additives, and 2) modification of polymer networks.

It is known that salt solutions exhibit depressed freezing points below 0 °C. For example, an aqueous solution with 23.3% of NaCl shows a suppressed freezing point of -21.1°C.[92] Therefore, salt is often used to melt ice and snow on pavements to prevent traffic accidents. Taking the advantage of freezing-depression by salt, Li et al. developed electrolyte hydrogel (EH) surfaces by introducing salts into poly(vinyl alcohol) hydrogel for anti-icing, as shown in Fig. 4a.[50] By tuning the concentration and species of salt, the EH surfaces demonstrate an ability to prevent ice/frost formation and reduce ice adhesion to Pascal-level even at a low temperature of -48.8 °C. Due to the ultralow ice adhesion, the formed ice on EH surface can be removed by gravity. Because the salt of EH can be replenished with various ion sources, e.g., seawater, the prepared EH surface shows great potential for applying on offshore infrastructure and ship hull. In addition to salts, many organic compounds, such as ethylene glycol, propylene glycol, glycerol, and dimethyl sulfoxide have also been utilized for freezing-point depression of water for cold environments, e.g., cryopreservation.[93, 94] Inspired by mollusks, which can secrete mucus to their skin surface to adapt to environmental change and protect themselves, Chen et al. prepared hydrogels containing large amount of cryoprotectants (CPTs, e.g., glycerol and ethylene glycol) via a solvent-displacement method (Fig. 4b).[51] The CPTs inside the gel matrix dynamically exchanged with the water and then melted the ice at the interface to form a liquid layer, which is highly favourable for both resisting frosting formation and facilitating low ice adhesion. Unfortunately, these anti-icing hydrogels continuously lose the crucial additives during usage, rendering their ultimate dysfunction in due time.

Based on the mobility and freezing temperatures of water, water molecules inside the hydrogels exist in one of the three states, i.e., unfrozen water, weakly bound water, and free water,[91, 95-97] depending on their interactions with polymer networks. Unfrozen water interacts strongly with polymer networks, thus possessing weak mobility and extremely low freezing temperature, even down to -100 °C. Weakly bound water has relatively low interaction with polymer matrix, their mobility is therefore partly restricted by the polymer network. Consequently, they can remain in amorphous state slightly below 0 °C. Free water is the water that has almost no interaction with polymer networks and shows the same freezing temperature as bulk water outside the hydrogel (~0 °C). Since the states of water in hydrogels highly depend on the interactions of water molecules with polymer segments, it is feasible to tune the water states by designing and modifying polymer networks.[2, 49, 53] Inspired by anti-freezing proteins, He et al. prepared PDMS-grafted polyelectrolyte hydrogel for anti-icing purpose.[2] As shown in Fig. 4c, by tuning the arrangement of hydrophobic PDMS and charged functional groups, the hydrogel can mimic the function of anti-freezing protein in maintaining an non-frozen interfacial water layer. The resulting interfacial water grants the hydrogel coating multifunctional anti-icing properties. The ice nucleation on the designed hydrogel surface is inhibited (ice nucleation temperature < -30 °C), because the optimized charge groups restrict the structural transformation of water from liquid-like to ice-like.[98] The ice propagation is also hindered by the altered ice-solution interfacial tension, which can be tuned by hydrophobic chains and ion species.[10, 66] The synergetic cooperation of hydrophobicity and ion specificity leads to effective restricted ice propagation rate.[2] In addition, the interfacial water can also serve as a lubricant to reduce the ice adhesion below 20 kPa. Altering crosslinking degree is another way to control the generation of interfacial water. In a fully hydrated hydrogel, the internal fraction of unfrozen water

increases with crosslinking degree because the internal polymer networks restrict the mobility of water molecules.[99-101] Huang et al. showed that the freezing temperature on a cross-linked hydrogel (cross-linked dopamine grafted sodium alginate, SA-g-DA) decreases with crosslinking degree.[49] Besides, crosslinking and grafting of dopamine grant the hydrogel with excellent stability and good adhesion on many types of solid surfaces, respectively.

In addition to bulk hydrogel coatings, surface-patterned hydrogels have been also designed for localized controlling of ice formation.[67, 100] Ice-nucleating proteins (INPs) found in many freeze-tolerant species promote ice nucleation in the extracellular spaces.[102, 103] The formed ice harvests water from the intracellular spaces due to lower vapor pressure of ice compared with that of water, which can prevent intracellular freezing.[100] Inspired by such freeze-tolerant organisms, patterned polyelectrolyte hydrogel (PH) surfaces[67] and patterned hydrogel-encapsulated INP (PHINP)[100] were developed, both displayed excellent ability to inhibit ice propagation. The ice nucleation temperature of hydrogel was increased by tuning the counterions of hydrogels or encapsulating INP into poly(acrylamide-co-2-hydroxyethyl methacrylate) hydrogels. As shown in Fig. 4d, the increased nucleation temperature leaded to the preferential formation of ice stripes on the coated area of the sample surface. Due to the lower vapour pressure over ice, the water vapour deposited on the formed ice. In addition, the latent heat was released to the substrate during freezing, facilitating the evaporation of neighbouring condensate water droplets. As a result, large ice-free zones can be achieved (Fig. 4d).[67, 100]

Although hydrogels mentioned above present excellent icephobicity, their functionality relies on the state of interfacial water, which is strongly affected by

temperature. At an extremely low temperature, it is challenging to keep the interfacial water at amorphous state.[11, 104]

3.3. Ionogels

Ionogels consist of polymer networks and ionic liquids. Thanks to the huge diversity of ionic liquids, the category of gels exhibits great versatility. By selecting various polymer networks and ionic liquids, ionogels have been widely utilized as self-cleaning surfaces,[105] stretchable ionic conductors,[106] electronic skins,[44] electrolytes for batteries,[45] and flexible supercapacitors.[46] According to their interaction with water, ionic liquids can be divided into hydrophilic and hydrophobic.[105] Although ionogels containing hydrophobic ionic liquids demonstrated excellent water repellency due to the lubrication effect,[105] their possible application in anti-icing field is surprisingly not reported. Hydrophilic ionic liquids are known for their capacity of freezing-point depression, which guarantees the corresponding ionogels as promising candidates for anti-icing application.[107] Zhuo et al. designed and prepared anti-icing ionogels consisting of crosslinked gelatin and 1-butyl-3-methylimidazolium bromide (BMImBr).[48] Due to the effective freezing-point depression of BMImBr, the ionogel surface can not only inhibit ice nucleation, but also alter the ice growth direction of the water droplets on the surface at sub-zero temperature. As shown in Fig. 4e, the unconventional inward ice growth from droplet-air interface to droplet-ionogel interface leads to a spherical cap ice rather than a normal pointy cap ice. Because of the inward growth and brine rejection at the freezing front, a concentrated ionic liquid aqueous layer can form at the ice-ionogel interface, enabling an ultralow ice adhesion. In addition, since the ionogel can absorb the water molecules even in cold environments to generate a non-frozen liquid layer on the surface, the prepared ionogel also exhibits remarkable anti-frost property. However,

the possible exhaustion of ionic liquid during application can result in the loss of icephobicity.

It is worth noting that the anti-icing application of ionogels is currently limited, because their anti-icing potentials started to be appreciated very recently and the leakage of some ionic liquids is hazardous to environment.[48] Nevertheless, such environmental issue could be overcome by using green ionic liquids. Given the great variety of both ionic liquids and polymers available, there is an almost unlimited number of combinations of the two for fabricating new anti-icing ionogels. In addition, the unique features of ionic liquids can bestow new functions on ionogels. For example, the high electrical conductivity of ionogels can be an ideal property for enabling electrothermal anti-icing and other electroresponsive potentials. As encouraging results further broadcasted,[48] ionogels can be as popular as, if not more favourite than, other two gel types for anti-icing.

4. Summary & perspective

In this review, we iterated the key events in icing and current anti-icing strategies to break the sequential chain of icing process firstly. We then surveyed the state-of-the-art gels that were designed and fabricated for anti-icing purpose. The current anti-icing gels were categorized into organogels, hydrogels, and ionogels for the convenience of referencing in future relevant studies. The comparison between these anti-icing gels is further outlined in Table 1. Overall, all the current anti-icing gels suffer from the common drawbacks of poor liquid retention ability, weak adhesion to substrate, low strength as well as low toughness. Most of organogels achieve anti-icing properties by incorporating interfacial lubricant layer to weaken the intrinsic adhesion. However, the liquid lubricant layer can be easily depleted, leading to a poor durability. To improve the

durability of anti-icing organogels, solid organogels, self-healing organogels, and thermoresponsive organogels can be developed. Interfacial water in hydrogels plays a crucial role in anti-icing performance.

Non-frozen water of hydrogels can be achieved by introducing additives or modifying polymer networks, resulting in a slippery surface for lowering ice adhesion. In addition, ice nucleation can be controlled by tuning charge groups in hydrogels. Bulk hydrogels that can inhibit ice nucleation and patterned hydrogels that can promote ice nucleation have been designed for anti-icing applications. However, the state of water is strongly influenced by temperature. At an extreme low temperature, it becomes highly challenging to keep the interfacial water at amorphous state.[11] The patterned hydrogels shows preferential formation of ice, and thus can harvest the water molecules from the atmosphere and the other surface area without hydrogels, and consequently lead to large ice-free zones. Anti-icing ionogels can not only inhibit ice nucleation but also alter the ice growth direction on their surface, which is enabled by the presence of ionic liquid and the resulting depressed freezing-point. In summary, despite that the current anti-icing gels still suffer from some major demerits, *i.e.*, poor durability, their remarkable anti-icing performances signify a promising future (Fig. 5a). In order to promote the development of gels-based anti-icing surfaces, we have identified the following paths for further research, including pathways to enhance durability, needs to build up the missing fundamentals, and possibility to enable stimuli responsive properties.

Durability. Weak durability of anti-icing gels results from the poor mechanical robustness, adhesive failure to substrate, and/or depletion of liquid phase or additives. The poor mechanical robustness of the current anti-icing gels roots in the low areal density of polymer strands and the missing of toughening strategy.[85] Fortunately, many

approaches have been developed to toughen polymer networks, such as incorporating energy dissipation networks, designing double networks, and adding fillers (Fig. 5b),[108] which can also be adopted to design tough and strong anti-icing gels.[2, 48] Another obvious challenge for anti-icing gel coatings is the weak adhesion to substrate due to the wet surfaces that resulted from the liquid phase of gel.[109, 110] The weak adhesion may be addressed by mimicking essential features of the adhesive chemistry practiced by mussels (Fig. 5c)[111] and/or designing topological adhesion (Fig. 5d).[112, 113]

In addition to the weak mechanical durability, the drain of liquid phase or additives is also key to the dysfunction of anti-icing gels. Due to the high fluidity, the liquid in gels may leak out, thus leading to the loss of anti-icing performance. The evaporation of the liquid part (especially water) will render the loss of functionality as well. Some gels diffuse functional molecules to the interface to achieve outstanding anti-icing performance, however, it comes with the cost of the diffused molecules being removed by water at the same time. Such process may not only be detrimental to long-term stability but also contaminative to the environment.[48, 91] Although replenishing salt from seawater has been adopted to improve the sustainability, the application condition of the corresponding gel was still limited to marine area.[50] Therefore, new advanced techniques should be developed for retaining liquid phase and additives. Developing polymer networks with high affinity to additives and immobilizing anti-freezing groups may mitigate the loss of functional component.

Fundamentals of anti-icing gels. In order to address the weak durability and maintain the outstanding anti-icing performances at the same time, it is vital to unravel and understand the fundamentals of anti-icing gels. In a previous work, the complex relationship between crosslinking density, water content and anti-icing properties of gels

has been investigated,[49] which provides clear guiding directions for future optimization and exploration of new anti-icing gels. Polymer brushes with various hydrophilic backbones and different length of hydrophobic side chains have been developed to mimic anti-freezing protein, and the relationship between molecular groups, water states and anti-icing performances has been studied.[2] Given that anti-icing gel is still in its infancy, the most urgent need would be to enlarge the sample populations and to enrich the corresponding anti-icing result database. Taking the anti-icing ionogels for example, accumulating a sufficiently large number of validated results can enable other powerful methodologies, such as machine learning, to participate in the relevant selection of ionic liquids. By doing so, concealed fundamentals of gels that are crucial to anti-icing can be revealed. Entangling puzzles, for example how the different polymer networks (linear including random and block, branched, cross-linked etc.) affect the water content (unfrozen water, weakly bound water, and free water) and thus anti-icing ability (Fig. 5e),[11, 114, 115] and how the functional groups (their species and grafting density) influence on the water states and anti-icing properties, can be solved.

External stimuli responsive properties. External stimuli responsive materials have attracted substantial attention thanks to their changeable properties towards various applications, e.g., responsive coatings, controllable liquid-repellency, adaptive shape memory materials.[116-118] Such external stimuli responsive properties can also endow the anti-icing gels with dynamic nature, instable interface, and thus reversible interaction with ice. In addition, on-demand response allows to reduce the loss of functional agent during usage and therefore enhance the durability. Hence, it is important to develop smart anti-icing gels. Unfortunately, only a few relevant studies on external stimuli responsive anti-icing gels have been reported until today. For example,

thermoresponsive property has been introduced into organogels to enhance the on-demand secreting of lubricant to the surface and to improve the anti-icing abilities and durability.[52, 86] It should be noted that not only temperature but also many other ambient conditions can serve as external stimuli. By designing polymer networks and incorporating nanoparticles, stress, light, electrical field, and magnetic field can also trigger changes in the gel properties (Fig. 5f).[117, 118] We envision that such smart anti-icing gels with predictable and changeable properties will widen the applications and hold great promise to address current defects.

Conflicts of interest

There are no conflicts to declare.

Acknowledgement

The Research Council of Norway is acknowledged for the support to the PETROMAKS2 Project Durable Arctic Icephobic Materials Project (No. 255507) and the Dandra Project (No. 302348). J. C. acknowledges the support by the National Natural Science Foundation of China (No. 21676133). T. L. thanks the support by the National Natural Science Foundation of China (No. 12002350), and the CAS Key Laboratory of Bio-inspired Materials and Interfacial Science, Technical Institute of Physics and Chemistry, Chinese Academy of Sciences.

References

1. K. Golovin, A. Dhyani, M. D. Thouless and A. Tuteja, *Science*, 2019, **364**, 371-375.
2. Z. Y. He, C. Y. Wu, M. T. Hua, S. W. Wu, D. Wu, X. Y. Zhu, J. J. Wang and X. M. He, *Matter*, 2020, **2**, 723-734.
3. Y. Shen, X. Wu, J. Tao, C. Zhu, Y. Lai and Z. Chen, *Progress in Materials Science*, 2019, **103**, 509-557.

4. Y. Zhuo, S. Xiao, A. Amirfazli, J. He and Z. Zhang, *Chemical Engineering Journal*, 2021, **405**, 127088.
5. S. Zhang, J. Huang, Y. Cheng, H. Yang, Z. Chen and Y. Lai, *Small*, 2017, **13**.
6. L. Mishchenko, B. Hatton, V. Bahadur, J. A. Taylor, T. Krupenkin and J. Aizenberg, *ACS Nano*, 2010, **4**, 7699-7707.
7. J. Chen, R. Dou, D. Cui, Q. Zhang, Y. Zhang, F. Xu, X. Zhou, J. Wang, Y. Song and L. Jiang, *ACS Appl Mater Interfaces*, 2013, **5**, 4026-4030.
8. R. Dou, J. Chen, Y. Zhang, X. Wang, D. Cui, Y. Song, L. Jiang and J. Wang, *ACS Appl Mater Interfaces*, 2014, **6**, 6998-7003.
9. H. Yang, C. Ma, K. Li, K. Liu, M. Loznik, R. Teeuwen, J. C. van Hest, X. Zhou, A. Herrmann and J. Wang, *Adv Mater*, 2016, **28**, 5008-5012.
10. Z. He, W. J. Xie, Z. Liu, G. Liu, Z. Wang, Y. Q. Gao and J. Wang, *Science advances*, 2016, **2**, e1600345.
11. J. Chen, Z. Luo, Q. Fan, J. Lv and J. Wang, *Small*, 2014, **10**, 4693-4699.
12. T. Cheng, R. He, Q. Zhang, X. Zhan and F. Chen, *Journal of Materials Chemistry A*, 2015, **3**, 21637-21646.
13. L. Wang, Q. Gong, S. Zhan, L. Jiang and Y. Zheng, *Adv Mater*, 2016, **28**, 7729-7735.
14. X. Gao and L. Jiang, *Nature*, 2004, **432**, 36.
15. M. Liu, S. Wang and L. Jiang, *Nature Reviews Materials*, 2017, **2**.
16. T. Maitra, M. K. Tiwari, C. Antonini, P. Schoch, S. Jung, P. Eberle and D. Poulikakos, *Nano Lett*, 2014, **14**, 172-182.
17. L. Cao, A. K. Jones, V. K. Sikka, J. Wu and D. Gao, *Langmuir*, 2009, **25**, 12444-12448.
18. V. Bahadur, L. Mishchenko, B. Hatton, J. A. Taylor, J. Aizenberg and T. Krupenkin, *Langmuir*, 2011, **27**, 14143-14150.
19. Y. Shen, J. Tao, H. Tao, S. Chen, L. Pan and T. Wang, *Langmuir*, 2015, **31**, 10799-10806.
20. M. Nosonovsky and V. Hejazi, *ACS Nano*, 2012, **6**, 8488-8491.
21. V. Hejazi, K. Sobolev and M. Nosonovsky, *Sci Rep*, 2013, **3**, 2194.
22. S. Bengaluru Subramanyam, V. Kondrashov, J. Ruhe and K. K. Varanasi, *ACS Appl Mater Interfaces*, 2016, **8**, 12583-12587.
23. A. M. Emelyanenko, L. B. Boinovich, A. A. Bezdomnikov, E. V. Chulkova and K. A. Emelyanenko, *ACS Appl Mater Interfaces*, 2017, **9**, 24210-24219.
24. L. B. Boinovich, A. M. Emelyanenko, K. A. Emelyanenko and E. B. Modin, *ACS Nano*, 2019, **13**, 4335-4346.
25. V. Vercillo, S. Tonnicchia, J. M. Romano, A. García‐Girón, A. I. Aguilar‐Morales, S. Alamri, S. S. Dimov, T. Kunze, A. F. Lasagni and E. Bonaccurso, *Advanced Functional Materials*, 2020, DOI: 10.1002/adfm.201910268, 1910268.
26. V. Vercillo, J. T. Cardoso, D. Huerta-Murillo, S. Tonnicchia, A. Laroche, J. A. Mayén Guillén, J. L. Ocaña, A. F. Lasagni and E. Bonaccurso, *Materials Letters: X*, 2019, **3**, 100021.
27. B. Liu, K. Zhang, C. Tao, Y. Zhao, X. Li, K. Zhu and X. Yuan, *RSC Advances*, 2016, **6**, 70251-70260.
28. G. Momen, R. Jafari and M. Farzaneh, *Applied Surface Science*, 2015, **349**, 211-218.
29. S. A. Kulinich, S. Farhadi, K. Nose and X. W. Du, *Langmuir*, 2011, **27**, 25-29.
30. T. S. Wong, S. H. Kang, S. K. Tang, E. J. Smythe, B. D. Hatton, A. Grinthal and J. Aizenberg, *Nature*, 2011, **477**, 443-447.
31. Y. Zhuo, F. Wang, S. Xiao, J. He and Z. Zhang, *ACS Omega*, 2018, **3**, 10139-10144.
32. M. J. Coady, M. Wood, G. Q. Wallace, K. E. Nielsen, A. M. Kietzig, F. Lagugne-Labarthet and P. J. Ragogna, *ACS Appl Mater Interfaces*, 2018, **10**, 2890-2896.

33. Q. Liu, Y. Yang, M. Huang, Y. Zhou, Y. Liu and X. Liang, *Applied Surface Science*, 2015, **346**, 68-76.
34. Y. Zhuo, V. Håkonsen, Z. He, S. Xiao, J. He and Z. Zhang, *ACS Appl Mater Interfaces*, 2018, **10**, 11972-11978.
35. Y. Zhuo, S. Xiao, V. Håkonsen, T. Li, F. Wang, J. He and Z. Zhang, *Applied Materials Today*, 2020, **19**, 100542.
36. Z. He, S. Xiao, H. Gao, J. He and Z. Zhang, *Soft Matter*, 2017, **13**, 6562-6568.
37. Z. He, Y. Zhuo, J. He and Z. Zhang, *Soft Matter*, 2018, **14**, 4846-4851.
38. Y. Zhuo, T. Li, F. Wang, V. Håkonsen, S. Xiao, J. He and Z. Zhang, *Soft Matter*, 2019, **15**, 3607-3611.
39. C. Jia, C. Chen, R. Mi, T. Li, J. Dai, Z. Yang, Y. Pei, S. He, H. Bian, S. H. Jang, J. Y. Zhu, B. Yang and L. Hu, *ACS Nano*, 2019, **13**, 9993-10001.
40. D. L. Beemer, W. Wang and A. K. Kota, *Journal of Materials Chemistry A*, 2016, **4**, 18253-18258.
41. K. Golovin, S. P. Kobaku, D. H. Lee, E. T. DiLoreto, J. M. Mabry and A. Tuteja, *Science advances*, 2016, **2**, e1501496.
42. X. Liu, J. Liu, S. Lin and X. Zhao, *Materials Today*, 2020, DOI: 10.1016/j.mattod.2019.12.026.
43. H. Fan and J. P. Gong, *Macromolecules*, 2020, **53**, 2769-2782.
44. Y. Cao, Y. J. Tan, S. Li, W. W. Lee, H. Guo, Y. Cai, C. Wang and B. C. K. Tee, *Nature Electronics*, 2019, **2**, 75-82.
45. G. Yang, Y. Song, Q. Wang, L. Zhang and L. Deng, *Materials & Design*, 2020, **190**, 108563.
46. C. Lu and X. Chen, *Acc Chem Res*, 2020, **53**, 1468-1477.
47. Z. Wang, J. Zhang, J. Liu, S. Hao, H. Song and J. Zhang, *ACS Applied Materials & Interfaces*, 2021, DOI: 10.1021/acsami.0c21121.
48. Y. Zhuo, S. Xiao, V. Håkonsen, J. He and Z. Zhang, *ACS Materials Letters*, 2020, **2**, 616-623.
49. B. Huang, S. Jiang, Y. Diao, X. Liu, W. Liu, J. Chen and H. Yang, *Molecules*, 2020, **25**, 3378.
50. T. Zhu, Y. Cheng, J. Huang, J. Xiong, M. Ge, J. Mao, Z. Liu, X. Dong, Z. Chen and Y. Lai, *Chemical Engineering Journal*, 2020, **399**, 125746.
51. F. Chen, Z. Xu, H. Wang, S. Handschuh-Wang, B. Wang and X. Zhou, *ACS Appl Mater Interfaces*, 2020, **12**, 55501-55509.
52. Y. Ru, R. Fang, Z. Gu, L. Jiang and M. Liu, *Angew Chem Int Ed Engl*, 2020, **59**, 11876-11880.
53. Q. Guo, Z. He, Y. Jin, S. Zhang, S. Wu, G. Bai, H. Xue, Z. Liu, S. Jin, L. Zhao and J. Wang, *Langmuir*, 2018, **34**, 11986-11991.
54. X. Yao, B. Chen, X. P. Morelle and Z. Suo, *Extreme Mechanics Letters*, 2021, **44**, 101225.
55. S. Nath, S. F. Ahmadi and J. B. Boreyko, *Nanoscale and Microscale Thermophysical Engineering*, 2016, **21**, 81-101.
56. N. Miljkovic, R. Enright, Y. Nam, K. Lopez, N. Dou, J. Sack and E. N. Wang, *Nano Lett*, 2013, **13**, 179-187.
57. Y. Long, X. Yin, P. Mu, Q. Wang, J. Hu and J. Li, *Chemical Engineering Journal*, 2020, **401**, 126137.
58. R. P. Sear, *Journal of Physics: Condensed Matter*, 2007, **19**, 033101.
59. T. M. Schutzius, S. Jung, T. Maitra, P. Eberle, C. Antonini, C. Stamatopoulos and D. Poulikakos, *Langmuir*, 2015, **31**, 4807-4821.
60. P. Eberle, M. K. Tiwari, T. Maitra and D. Poulikakos, *Nanoscale*, 2014, **6**, 4874-4881.

61. G. Bai, D. Gao, Z. Liu, X. Zhou and J. Wang, *Nature*, 2019, **576**, 437-441.
62. O. R. Enríquez, Á. G. Marín, K. G. Winkels and J. H. Snoeijer, *Physics of Fluids*, 2012, **24**, 091102.
63. G. Graeber, T. M. Schutzius, H. Eghlidi and D. Poulikakos, *Proc Natl Acad Sci U S A*, 2017, **114**, 11040-11045.
64. J. Liu, C. Zhu, K. Liu, Y. Jiang, Y. Song, J. S. Francisco, X. C. Zeng and J. Wang, *Proc Natl Acad Sci U S A*, 2017, **114**, 11285-11290.
65. S. Jung, M. K. Tiwari and D. Poulikakos, *Proc Natl Acad Sci U S A*, 2012, **109**, 16073-16078.
66. Y. Jin, Z. He, Q. Guo and J. Wang, *Angew Chem Int Ed Engl*, 2017, **56**, 11436-11439.
67. Y. Jin, C. Wu, Y. Yang, J. Wu, Z. He and J. Wang, *ACS Nano*, 2020, DOI: 10.1021/acsnano.0c01304.
68. S. Nath and J. B. Boreyko, *Langmuir*, 2016, **32**, 8350-8365.
69. S. F. Ahmadi, S. Nath, G. J. Iliff, B. R. Srijanto, C. P. Collier, P. Yue and J. B. Boreyko, *ACS Appl Mater Interfaces*, 2018, **10**, 32874-32884.
70. Y. Yao, T. Y. Zhao, C. Machado, E. Feldman, N. A. Patankar and K. C. Park, *Proc Natl Acad Sci U S A*, 2020, **117**, 6323-6329.
71. Y. Zhao, Z. Yan, H. Zhang, C. Yang and P. Cheng, *International Journal of Heat and Mass Transfer*, 2021, **165**, 120609.
72. L. A. Wilen, J. S. Wettlaufer, M. Elbaum and M. Schick, *Phys Rev B Condens Matter*, 1995, **52**, 12426-12433.
73. I. A. Ryzhkin and V. F. Petrenko, *The Journal of Physical Chemistry B*, 1997, **101**, 6267-6270.
74. S. Xiao, J. He and Z. Zhang, *Nanoscale*, 2016, **8**, 14625-14632.
75. S. Xiao, B. H. Skallerud, F. Wang, Z. Zhang and J. He, *Nanoscale*, 2019, **11**, 16262-16269.
76. A. J. Meuler, J. D. Smith, K. K. Varanasi, J. M. Mabry, G. H. McKinley and R. E. Cohen, *ACS Appl Mater Interfaces*, 2010, **2**, 3100-3110.
77. Z. He, E. T. Vagenes, C. Delabahan, J. He and Z. Zhang, *Sci Rep*, 2017, **7**, 42181.
78. Y. Li, C. Luo, X. Li, K. Zhang, Y. Zhao, K. Zhu and X. Yuan, *Applied Surface Science*, 2016, **360**, 113-120.
79. P. Juuti, J. Haapanen, C. Stenroos, H. Niemelä-Anttonen, J. Harra, H. Koivuluoto, H. Teisala, J. Lahti, M. Tuominen, J. Kuusipalo, P. Vuoristo and J. M. Mäkelä, *Applied Physics Letters*, 2017, **110**.
80. P. Kim, T. S. Wong, J. Alvarenga, M. J. Kreder, W. E. Adorno-Martinez and J. Aizenberg, *ACS Nano*, 2012, **6**, 6569-6577.
81. H. Yao and H. Gao, *Journal of Computational and Theoretical Nanoscience*, 2010, **7**, 1299-1305.
82. P. Irajizad, A. Al-Bayati, B. Eslami, T. Shafquat, M. Nazari, P. Jafari, V. Kashyap, A. Masoudi, D. Araya and H. Ghasemi, *Materials Horizons*, 2019, **6**, 758-766.
83. Y. L. Wang, X. Yao, J. Chen, Z. Y. He, J. Liu, Q. Y. Li, J. J. Wang and L. Jiang, *Sci China Mater*, 2015, **58**, 559-565.
84. C. Urata, G. J. Dunderdale, M. W. England and A. Hozumi, *Journal of Materials Chemistry A*, 2015, **3**, 12626-12630.
85. C. Creton, *Macromolecules*, 2017, **50**, 8297-8316.
86. C. Urata, R. Hönes, T. Sato, H. Kakiuchida, Y. Matsuo and A. Hozumi, *Advanced Materials Interfaces*, 2019, **6**, 1801358.
87. A. Sandhu, O. J. Walker, A. Nistal, K. L. Choy and A. J. Clancy, *Chem Commun (Camb)*, 2019, **55**, 3215-3218.
88. Y. Wang, X. Yao, S. Wu, Q. Li, J. Lv, J. Wang and L. Jiang, *Adv Mater*, 2017, **29**.

89. G. M. Chen, S. C. Liu, Z. Y. Sun, S. F. Wen, T. Feng and Z. F. Yue, *Progress in Organic Coatings*, 2020, **144**, 105641.
90. Y. Yu, B. Jin, M. I. Jamil, D. Cheng, Q. Zhang, X. Zhan and F. Chen, *ACS Appl Mater Interfaces*, 2019, **11**, 12838-12845.
91. Y. Jian, S. Handschuh-Wang, J. Zhang, W. Lu, X. Zhou and T. Chen, *Materials Horizons*, 2020, DOI: 10.1039/d0mh01029d.
92. M. M. Conde, M. Rovere and P. Gallo, *Journal of Molecular Liquids*, 2018, **261**, 513-519.
93. S. S. N. Murthy, *Cryobiology*, 1998, **36**, 84-96.
94. T. Chang and G. Zhao, *Advanced Science*, 2021, DOI: 10.1002/advs.202002425, 2002425.
95. S. Cerveny, J. Colmenero and A. Alegría, *Macromolecules*, 2005, **38**, 7056-7063.
96. V. Gun'ko, I. Savina and S. Mikhalovsky, *Gels*, 2017, **3**, 37.
97. S. V. Elgersma, M. Ha, J. J. Yang, V. K. Michaelis and L. D. Unsworth, *Materials (Basel)*, 2019, **12**.
98. Z. He, K. Liu and J. Wang, *Acc Chem Res*, 2018, **51**, 1082-1091.
99. W. Borchard, A. Kenning, A. Kapp and C. Mayer, *Int J Biol Macromol*, 2005, **35**, 247-256.
100. Z. Wang, B. Lin, S. Sheng, S. Tan, P. Wang, Y. Tao, Z. Liu, Z. He and J. Wang, *CCS Chemistry*, 2021, DOI: 10.31635/ccschem.021.202000648, 1-23.
101. P. McConville and J. M. Pope, *Polymer*, 2001, **42**, 3559-3568.
102. M. R. Michaud and D. L. Denlinger, *International Congress Series*, 2004, **1275**, 32-46.
103. R. A. Brush, M. Griffith and A. Mlynarz, *Plant Physiol*, 1994, **104**, 725-735.
104. F. Wang, S. B. Xiao, Y. Z. Zhuo, W. W. Ding, J. Y. He and Z. L. Zhang, *Materials Horizons*, 2019, **6**, 2063-2072.
105. Y. Ding, J. Zhang, X. Zhang, Y. Zhou, S. Wang, H. Liu and L. Jiang, *Advanced Materials Interfaces*, 2015, **2**, 1500177.
106. Y. Cao, T. G. Morrissey, E. Acome, S. I. Allec, B. M. Wong, C. Keplinger and C. Wang, *Adv Mater*, 2017, **29**.
107. Y. Liu, A. S. Meyer, Y. Nie, S. Zhang, Y. Zhao, P. L. Fosbøl and K. Thomsen, *Journal of Chemical & Engineering Data*, 2017, **62**, 2374-2383.
108. Y. Huang, L. Xiao, J. Zhou, X. Li, J. Liu and M. Zeng, *J Mater Sci*, 2020, **55**, 14690-14701.
109. J. Li, A. D. Celiz, J. Yang, Q. Yang, I. Wamala, W. Whyte, B. R. Seo, N. V. Vasilyev, J. J. Vlassak, Z. Suo and D. J. Mooney, *Science*, 2017, **357**, 378-381.
110. X. Yao, J. Liu, C. Yang, X. Yang, J. Wei, Y. Xia, X. Gong and Z. Suo, *Adv Mater*, 2019, **31**, e1903062.
111. B. P. Lee, P. B. Messersmith, J. N. Israelachvili and J. H. Waite, *Annu Rev Mater Res*, 2011, **41**, 99-132.
112. J. Steck, J. Yang and Z. Suo, *ACS Macro Letters*, 2019, **8**, 754-758.
113. J. Yang, R. Bai and Z. Suo, *Adv Mater*, 2018, **30**, e1800671.
114. W. D. Callister Jr and D. G. Rethwisch, *Fundamentals of materials science and engineering: an integrated approach*, John Wiley & Sons, 2020.
115. Z. Li, Z. Liu, T. Y. Ng and P. Sharma, *Extreme Mechanics Letters*, 2020, **35**, 100617.
116. P. Theato, B. S. Sumerlin, R. K. O'Reilly and T. H. Epps, 3rd, *Chem Soc Rev*, 2013, **42**, 7055-7056.
117. X. Yang, Y. Huang, Y. Zhao, X. Zhang, J. Wang, E. E. Sann, K. H. Mon, X. Lou and F. Xia, *Front Chem*, 2019, **7**, 826.
118. L. Hu, Y. Wan, Q. Zhang and M. J. Serpe, *Advanced Functional Materials*, 2019, **30**, 1903471.

1

Figures

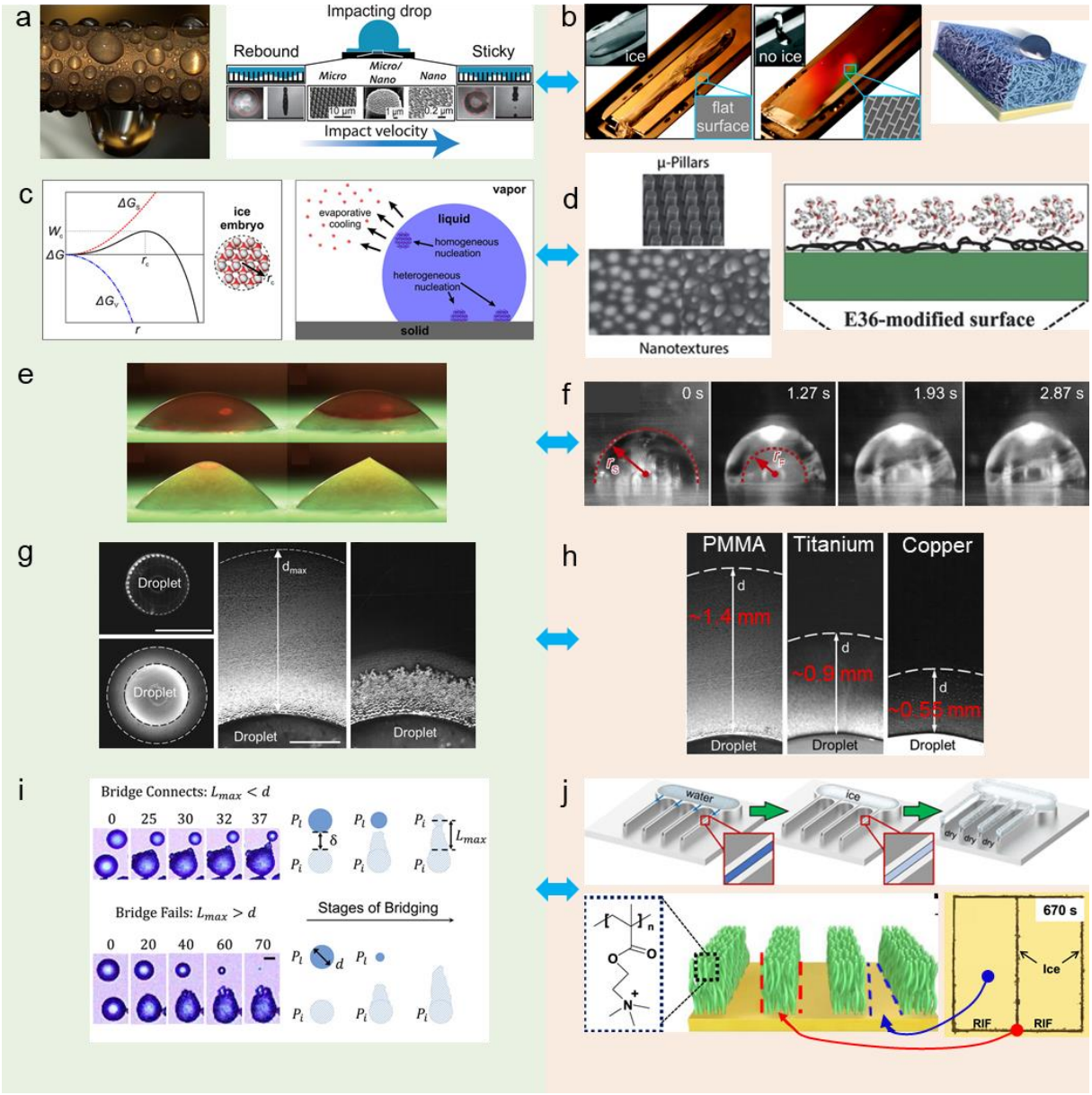

Fig. 1. From icing process (left, light green background) to anti-icing strategies (right, light orange background). (a) Collection of water via condensation[56] (left; copyright 2013 American Chemical Society) and adhesion of impacting droplets[16] (right; copyright 2014 American Chemical Society). (b) Repelling water droplets by using nanostructured SHS[6] (left, copyright 2010, American Chemical Society) and LIS[30] (right, copyright 2011 Springer Nature). (c) Ice nucleation.[59] Copyright 2015 American Chemical Society. (d) Inhibiting ice nucleation by designing nanostructured surface (left,

copyright 2014 Royal Society of Chemistry) and supercharged polypeptides surface (right, copyright 2016 Wiely-VCH). (e) Ice growth and recrystallization.[62] Copyright 2012 American Institute of Physics. (f) Inwards growth of ice induces spontaneous self-dislodging of droplets.[63] Copyright 2017 National Academy of Sciences. (g) Frost halos.[65] Copyright 2012 National Academy of Sciences. (h) Maximum expanse of PMMA, titanium, and copper under 1.3% humidity.[65] Copyright 2012 National Academy of Sciences. (i) Interdroplet ice bridging and dry zones.[68] Copyright 2016 American Chemical Society. (j) Restricting ice propagation by using microscopic ice patterns[69] (top, copyright 2018 American Chemical Society) and grafting patterned polyelectrolyte[67] (bottom, copyright 2020 American Chemical Society).

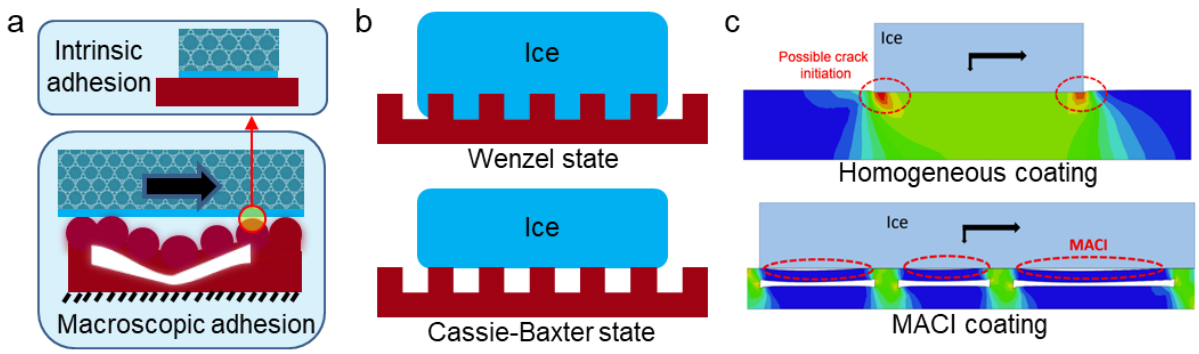

Fig. 2. Ice adhesion mechanics. (a) Intrinsic ice adhesion and macroscopic ice adhesion.[4] Copyright 2021 Elsevier. (b) Wenzel state and Cassie-Baxter state ice. Wenzel state ice forms mechanical interlocking with surface. (c) Cracks induced by interfacial inhomogeneity. MACI: Macrocrack initiators.[36] Copyright 2017 Royal Society of Chemistry.

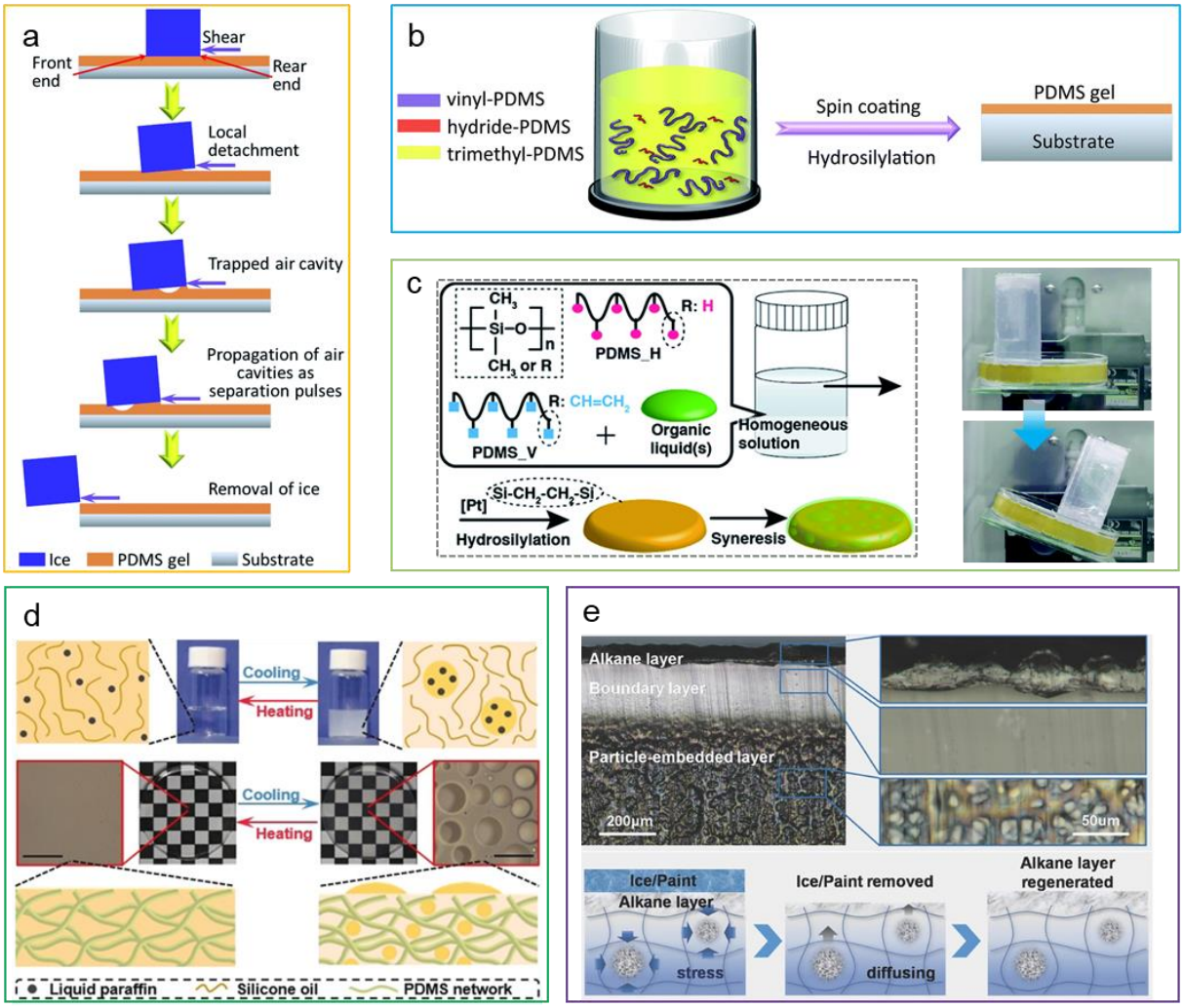

Fig. 3. Anti-icing organogels. (a) Formation of cavities at the interface between ice and soft organogels during deicing.[40] Copyright 2016 Royal Society of Chemistry. (b) Preparation of PDMS organogels.[40] Copyright 2016 Royal Society of Chemistry. (c) Crosslinking syneresis of PDMS induces secretion of organic liquids, enabling autonomous sliding off of ice on a slightly inclined surface.[84] Copyright 2015 Royal Society of Chemistry. (d) Phase separation of liquid paraffin/silicone oil solution and phase separation of reversibly thermosecreting organogels.[52] Copyright 2020 Wiely-VCH. (e) Solid organogels with a regenerable sacrificial alkane surface layer.[88] Copyright 2017 Wiely-VCH.

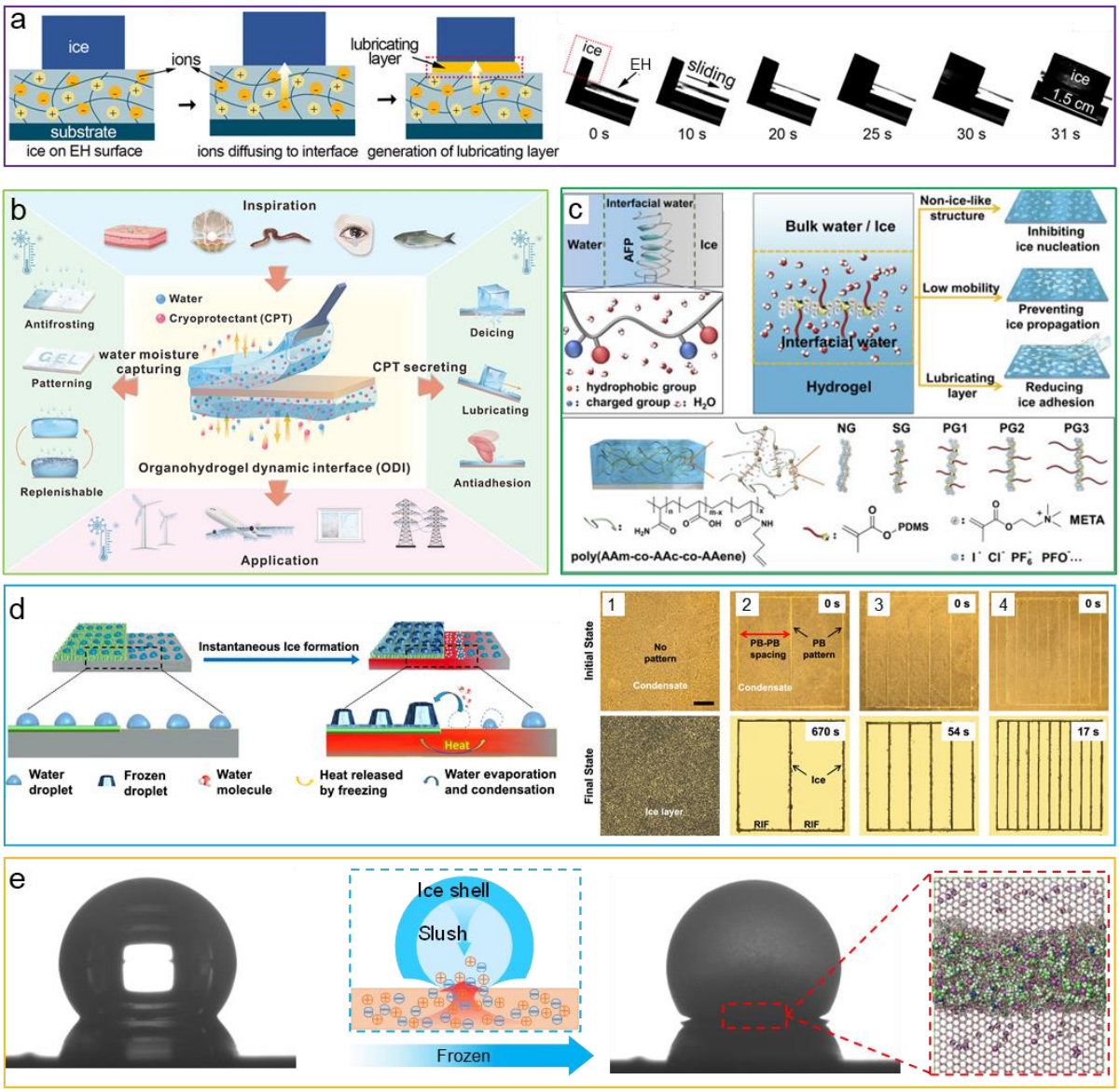

Fig. 4. Anti-icing hydrogels and ionogels. (a) Electrolyte hydrogel surfaces melt the ice at the interface to form a lubricating layer, which enables the automatic sliding off of ice.[50] Copyright 2020 American Chemical Society. (b) Hydrogels consist of CPTs inspired by mucus secretion towards applications at sub-zero temperature.[51] Copyright 2020 American Chemical Society. (c) Bioinspired multifunctional anti-icing hydrogel.[2] Copyright 2020 Elsevier. (d) Patterned hydrogel surface prevents the propagation of ice, resulting in large ice-free zones.[67] Copyright 2020 American Chemical Society. (e) Unconventional inward ice growth on ionogel surfaces leads to a spherical cap and a

concentrated ionic liquid aqueous interface.[48] Copyright 2020 American Chemical Society.

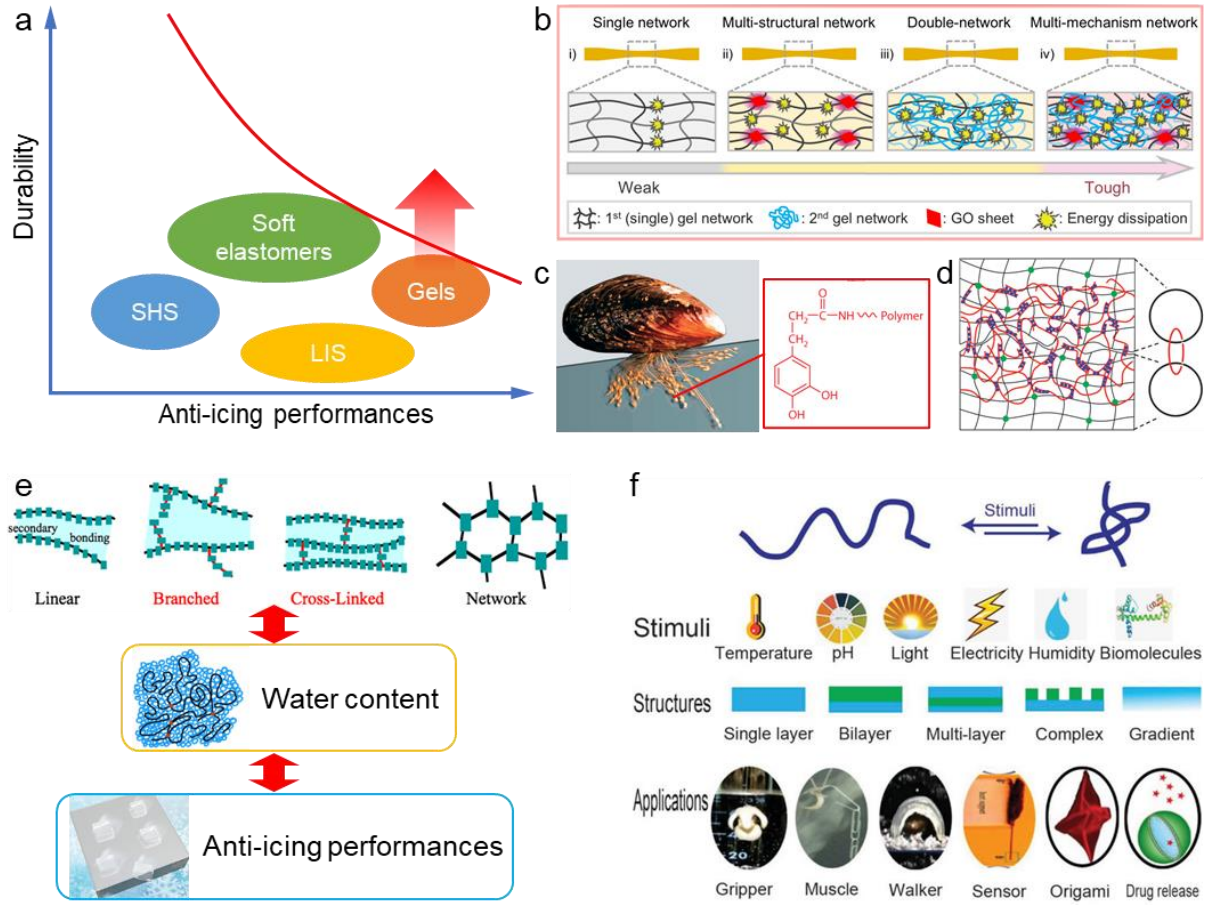

Fig. 5. Perspectives of anti-icing gels. (a) Anti-icing performances and durability of current anti-icing materials denote the improving direction of anti-icing gels. (b) Toughening strategies of gels by introducing 2nd network, nanofillers and energy dissipation mechanism.[108] Copyright 2020 Springer Nature. (c) Enhancing the adhesion of gels to substrates by mimicking essential features of the adhesive chemistry practiced by mussels.[111] Copyright 2001 ANNUAL REVIEWS. (d) Designing topological networks to increase the adhesion between gels and dry polymer.[113] Copyright 2018 Wiely-VCH.(e) The relationships between polymer networks, water content and anti-icing performances are awaiting to be discovered.[11, 114, 115] Copyright 2020 Elsevier & 2014 Wiely-VCH. (f) The changeable properties of stimuli responsive materials support various applications.[118] By incorporating external stimuli responsive properties into anti-icing gels will widen the applications and hold great promise to address current defects. Copyright 2019 Wiely-VCH.

Table 1. Comparison of different types of anti-icing gels.

Materials	Major contents	Mechanisms	Drawbacks	
			Individual	**Common**
Organogels	Organic compound	Deformation incompatibility	Limited application scenarios, e.g., deformation of coating can dramatically increase the unwanted drag force of wind turbine, aircraft, and ship hull	Poor liquid retention ability; weak adhesion to substrates; low strength; low toughness
		Lubrication	Easy to be evaporated and drained away; environmental unfriendly	
Hydrogels	Water	Freezing point depression additives	Additives are easy to be removed away; environmental unfriendly	
		Interfacial water control by network design	Strong temperature dependence	
Ionogels	Ionic liquid	Freezing point depression	Ionic liquids are easy to be removed by water; environmental unfriendly	